Title
POTENTIAL ENERGY SURFACES RELATED TO THE ION-MOLECULE REACTION C+ + H2

Authors
Liskow, Dean H.
Bender, Charles F.
Schaefer, Henry F.

Publication Date
1973-10-01

Submitted to Journal
of Chemical Physics

LBL-2302
Preprint

POTENTIAL ENERGY SURFACES RELATED TO THE ION-MOLECULE REACTION $C^+ + H_2$

Dean H. Liskow, Charles F. Bender
and Henry F. Schaefer III

October 1973

Prepared for the U. S. Atomic Energy Commission
under Contract W-7405-ENG-48

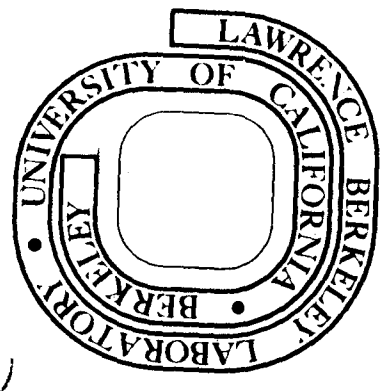

LBL-2302

DISCLAIMER

POTENTIAL ENERGY SURFACES RELATED TO THE ION-MOLECULE REACTION $C^+ + H_2$*

Dean H. Liskow, Charles F. Bender†, and Henry F. Schaefer III††

Department of Chemistry and
Lawrence Berkeley Laboratory
University of California
Berkeley, California 94720

October 1973

ABSTRACT

The $C^+ + H_2$ ion-molecule reaction has been studied by several experimental groups and appears destined to become the focal point of much experimental and theoretical activity. Ab initio self-consistent-field and configuration interaction calculations have accordingly been carried out for this system. A double zeta basis set of contracted gaussian functions was employed and as many as 570 configurations included. For isosceles triangle configurations (C_{2V} point group) the $^2A_1$, $^2B_1$, and $^2B_2$ potential surfaces were considered, while for linear geometries ($C_{\infty V}$) the $^2\Sigma^+$ and $^2\Pi$ surfaces were studied. Properties reported include minimum energy paths and energy profiles for the various processes considered. The intuitive correlation diagram of Mahan and Sloane is made semiquantitative in reliability. Pathways to CH_2^+ complex formation will depend crucially on the C_S potential surface.

INTRODUCTION

One of the primary motivations for molecular beam studies of ion-molecule reactions has been the hope of learning something about the potential energy surface or surfaces upon which the reaction occurs.[1] A closely related question is that of whether a reaction proceeds via an intermediate complex (of lifetime equal to several rotational periods) or by a direct mechanism.[2] The most obvious requirement for complex formation is that there exist a potential well along the reaction pathway.

Therefore it is not surprising that among the most intriguing ion-molecule reactions are those for which neither the "complex" nor "direct" label is entirely appropriate. One such example is the extensively studied[3-7] reaction $C^+ + H_2 \rightarrow CH^+ + H$. Koski and coworkers[4,6] found product angular distributions which were essentially symmetric at relative energies less than 4.4 eV, and concluded that complex formation was important in this region. It is well known[8,9] that there are two bound, low-lying electronic states of CH_2^+, the $^2A_1$ state with bond angle $\sim 140^\circ$ and the linear $^2\Pi(^2B_1)$ state, which lies at ~ 0.14 eV = 3.3 kcal/mole. Lindemann et al.[6] were also able to obtain a threshold value of 0.4 ± 0.1 eV for the reaction. Since $C^+ + H_2 \rightarrow CH^+ + H$ is endothermic by ~ 0.4 eV = 9 kcal/mole,[7] this amounts to a statement that the reaction proceeds without a barrier or activation energy. This would appear to be a reasonable finding, since many ion-molecule reactions are known to have zero activation energy.

In a paper describing molecular orbital correlation diagrams as they relate to ion-molecule reactions, Mahan[5] has shown that, for C_{2V} approaches of C^+ to H_2, the bound $^2A_1$ and $^2B_1$ electronic states are inaccessible in the sense of the Woodward-Hoffmann rules. That is, the $^2A_1$ and $^2B_1$ electron

configurations for separated $C^+ + H_2$ each differ by two electrons from the configurations for the bound $^2A_1$ and $^2B_1$ states. In addition Mahan[5] noted, as Wolfgang[2] has also discussed, that symmetric product angular distributions are a necessary but not sufficient criterion for complex formation.

Very recently, Mahan and Sloane[7] have completed the most complete beam study to date of the $C^+ + H_2$ reaction. They concluded that at relative energies below 4 eV a complex of lifetime comparable to one rotational period is formed. We have italicized the word one to emphasize the point that complex formation is usually associated with lifetimes of several rotational periods. Mahan and Sloane's conclusion was based on a) a high, but not perfect, degree of symmetry in the product velocity distribution; b) the similarity in the isotopic product velocity vector distributions from the reactions of C^+ with H_2, HD, and D_2; c) a very inelastic component in the non-reactively scattered C^+ ions.

Our interest in $C^+ + H_2$ is motivated by a feeling that this reaction will play a crucial role in the development of an understanding of the potential surfaces and dynamics associated with simple ion-molecule reactions. In this sense we feel that $C^+ + H_2$ will play a role comparable to that which $F + H_2$ has played[11-17] for neutral A + BC reactions. From a theoretical point of view, the primary difference between the two systems is that, while the dynamics of the $F + H_2$ system can for the most part be described in terms of a single potential energy surface, the $C^+ - H_2$ reaction involves several potential surfaces. This is perhaps best seen from the correlation diagram of Mahan and Sloane,[7] which diagram we have reproduced in Fig. 1.

The last section of the paper by Mahan and Sloane is devoted to a fascinating, if somewhat speculative, discussion of the relationship between

the molecular beam observations and the possible shapes of the $C^+ - H_2$ potential energy surfaces. The primary task facing them was to explain the apparently significant amount of complex formation despite the Woodward-Hoffmann "forbiddenness" of getting to the two low-lying bound states of CH_2^+. Central to their discussion is the fact that several surface crossings (e.g. $^2B_2$ with $^2A_1$) become avoided intersections for general C_S geometries. For example, the $^2B_2$ and $^2A_1$ states are both of $^2A'$ symmetry for point group C_S. Hence they argue that one can, and frequently will, proceed adiabatically from $C^+ + H_2$ to the ground and first excited electronic states of CH_2^+.

In the present paper we present the results of an ab initio study designed to test the qualitative accuracy of Fig. 1, and to resolve several other points raised by Mahan and Sloane in their discussion. We should say from the outset, however, that the potential surfaces alone do not tell the entire story. For example, it is certainly possible to proceed adiabatically from $C^+ + H_2$ to $^2A_1$ CH_2^+. However, whether this in fact will occur to any substantial degree depends not only on the nature of the avoided intersection, but also on the accompanying dynamics.[18] This is one of the reasons for our suspicion that the $C^+ + H_2$ reaction will continue to be of broad theoretical interest for some time to come.

THEORETICAL APPROACH

The present quantum mechanical calculations were designed to be comparable in quality to those previously reported[9] for the $^2A_1$ and $^2B_1$ bound states. As before, the Huzinaga-Dunning[19,20] C(9s 5p/4s 2p), H(4s/2s) basis set of contracted gaussian functions was used.

Since the earlier study was restricted to geometries near equilibrium, a configuration interaction (CI) for the $^2A_1$ ground state was carried out including all singly- and doubly-excited configurations with respect to the self-consistent-field (SCF) configuration

$$1a_1^2\ 2a_1^2\ 1b_2^2\ 3a_1 \qquad (1)$$

with the restriction that the $1a_1$ orbital was always doubly-occupied. For such geometries, this type of CI is nearly equivalent to full valence configuration interaction. More precisely, such a calculation should recover 95-99% of the valence shell correlation energy attainable with the chosen basis set.[21] However, for large $C^+ - H_2$ separations, the wave function will be dominated by a different reference configuration

$$1a_1^2\ 2a_1^2\ 3a_1^2\ 4a_1 \qquad (2)$$

and the above-described CI will not be comparable to full CI. Therefore, to describe both regions of the potential surface equally well, we have included all single and double excitations with respect to both reference configurations (1) and (2). Finally, a third reference configuration

$$1a_1^2\ 2a_1^2\ 1b_1^2\ 3a_1 \qquad (3)$$

was added for completeness. In this way, there are 570 configurations included in the $^2A_1$ calculations.

An analogous situation holds for the $^2B_1$ state. For large $C^+ - H_2$ separations, the single configuration

$$1a_1^2\ 2a_1^2\ 3a_1^2\ 1b_1 \tag{4}$$

is appropriate, but near equilibrium (r(CH) $\sim$ 1.09 Å, $\theta = 180°$) the wave function is well described by

$$1a_1^2\ 2a_1^2\ 1b_2^2\ 1b_1 \tag{5}$$

Note that the reason the deep well of the $^2B_1$ state is inaccessible in the sense of Woodward and Hoffmann[10] is the fact that $C^+ + H_2$ collisions must "switch" (via an avoided intersection) from configuration (4) to configuration (5). For a proper description of the entire potential surface we have constructed a 380 configuration wave function which includes all single and double excitations with respect to both reference states (4) and (5).

The $^2B_2$ state is simpler to describe, since a single configuration

$$1a_1^2\ 2a_1^2\ 3a_1^2\ 1b_2 \tag{6}$$

is appropriate for both limiting regions. All single and double excitations with respect to (6) provides our 262 configuration wave function. Note that the previous study[9] did not include this state, since it is expected to lie higher than the $^2A_1$ and $^2B_1$ states. It is also worth mentioning that Walsh's diagram[22] for AH_2 molecules can be used to predict this $^2B_2$ state to be strongly bent, slightly more so than $^1A_1$ CH_2, whose bond angle is known[23] to be 102.4°.

For linear nonsymmetric (CHH) geometries, $C^+ + H_2$ collisions can occur on $^2\Sigma^+$ or $^2\Pi$ potential energy surfaces (see Fig. 1). The $^2\Sigma^+$ surface is particularly simple for us to describe since a single configuration

$$1\sigma^2\ 2\sigma^2\ 3\sigma^2\ 4\sigma \tag{7}$$

describes both $C^+ + H_2$ and $CH^+(^1\Sigma^+) + H$ quite well. All single and double excitations with respect to (7) yield a CI of order 338. The $^2\Pi$ case is more difficult since the configuration which suffices for $C^+ + H_2$

$$1\sigma^2\ 2\sigma^2\ 3\sigma^2\ 1\pi \tag{8}$$

differs from that required for a minimal description of $CH^+(^3\Pi) + H$

$$1\sigma^2\ 2\sigma^2\ 3\sigma\ 1\pi\ 4\sigma \quad . \tag{9}$$

Thus it was necessary to include all single and double excitations with respect to both (7) and (8), for a total of 569 configurations.

In each of the five types ($^2A_1$, $^2B_1$, $^2B_2$, $^2\Sigma^+$, and $^2\Pi$) of calculation, a single configuration SCF calculation was first performed. Then the CI was repeated several times, the natural orbitals from the previous iteration being used in each calculation.[24,25]

GEOMETRIES CONSIDERED

Figures 2 and 3 show the coordinate systems adopted for the C_{2V} and $C_{\infty V}$ point group calculations. Note that for C_{2V} geometries R is the distance between the carbon nucleus and the H_2 midpoint, but for $C_{\infty V}$ geometries R is the C - H internuclear distance. In both cases r is the H - H separation.

Our goal in the present work has not been to fully map out the five two-dimensional potential energy surfaces. Rather we have restricted ourselves to the task of identifying a few key features of these surfaces, including a) the barrier heights in going from $C^+ + H_2$ to the CH_2^+ bound states and b) for linear CHH approach, the barriers to formation of $CH^+ (^2\Sigma$ and $^2\Pi) + H$. In addition, some information about minimum energy paths was desired. Thus the geometries considered were picked by a trial and error procedure. The computed total energies are given in an appendix, contained in our complete report[26] of this research.

REACTANTS AND PRODUCTS

The total and relative energies of $C^+ + H_2$, CH_2^+, and $CH^+ + H$ are given in Table I. First we look at the exothermicity for $C^+ + H_2 \rightarrow CH^+ + H$. The experimental value for this quantity is 0.44 eV = 10.1 kcal/mole, obtained by subtracting the dissociation energy of CH^+ (D_o = 4.04 eV[27]) from that of H_2 (D_o = 4.48 eV[28]). However, the classical exothermicity we have calculated [$E(C^+ + H_2) - E(CH^+ + H)$] corresponds to the difference in D_e values for CH^+ (4.21 eV) and H_2 (4.75 eV) and hence is 0.54 eV = 12.5 kcal/mole. The theoretical value in Table I, +20.8 kcal/mole, is then seen to be 8.3 kcal/mole larger than experiment.

Although the $^1\Sigma^+ - {}^3\Pi$ separation in CH^+ is not known experimentally, there is the accurate theoretical value 1.14 eV = 26.3 kcal/mole of Green, Bagus, Liu, McLean, and Yoshimine.[29] This theoretical value is probably within 4 kcal/mole of the exact result. For the same T_e value, the present theoretical calculations yield a value of 18.3 kcal/mole, 8 kcal below the more reliable result. Earlier calculations by Moore, Browne, and Matsen[30] gave a $^1\Sigma^+ - {}^3\Pi$ splitting of 14 kcal/mole.

Table I emphasizes the large potential wells (82 and 79 kcal/mole deep) which may be accessible to $C^+ - H_2$ collisions. However, it is also seen that there is no chemical well associated with the $^2B_2$ state. The only potential well for the $^2B_2$ state is that due to the long range attraction between C^+ and H_2. And in fact this well occurs for R = 3.34 bohrs, r = 1.49 bohrs, i.e. for rather large $C^+ - H_2$ separations. Further, the present calculations predict that there is no bound $^2B_2$ state at the geometry expected from chemical intuition (C - H distance 1.1 Å) and Walsh's rules ($\theta \leqslant 102°$). A

calculation carried out at the expected geometry yielded a total energy -38.4058 hartrees, or 49 kcal/mole repulsive relative to separated $C^+ + H_2$.

C_{2V} APPROACHES

The stationary points (other than separated $C^+ + H_2$) for C_{2V} geometries are shown in Table II. Notice first the $^2B_2$ long range attraction mentioned in the previous paragraph. The $^2B_1$ state has a qualitatively similar 7.3 kcal/mole well, but it occurs for a geometry somewhat closer (R is larger, r is smaller) to the reactants. There is no evidence of an attraction of this magnitude for the $^2A_1$ state. This of course does not preclude the possibility of a smaller ($\leqslant$ 1 kcal/mole) attraction for larger R values ($\geqslant$ 5 bohrs) than considered here.

Table II shows that very large barriers accompany the C_{2V} formation of the $^2A_1$ and $^2B_1$ states of CH_2^+. These barriers represent an ab initio verification of Woodward and Hoffman's qualitative concept of conservation of electron configuration. The electron configurations for $C^+ + H_2$ differ by two electrons ($b_2^2 \rightarrow a_1^2$) from those for CH_2^+.

More information related to these barriers is given in Table III and Fig. 4. Table III maps out the minimum energy paths for $C^+ + H_2 \rightarrow CH_2^+$ near the saddle points. The saddle points were located by the stationary condition

$$\frac{\partial V}{\partial R} = \frac{\partial V}{\partial r} = 0$$

and the minimum energy paths were found by following the gradient (reduced mass weighted) of the energy in its most negative direction. Figure 4 shows the energy profiles for the $C^+ + H_2$ C_{2V} approaches. As mentioned previously and illustrated clearly in Fig. 4, there is not a bound $^2B_2$ state of CH_2^+.

The fact that the $^2A_1$ barrier occurs "closer" in the sense of Hammond[31] to the reactants is nicely illustrated in Fig. 4. This is also seen in

Tables II and III, where the H - H distance at the $^2A_1$ saddle point is seen to be 0.66 bohrs shorter than that for the $^2B_1$ state. For the $^2A_1$ state, the minimum energy path near the saddle point shows a relatively large change (0.50 bohrs) in the H - H separation accompanied by a change of only 0.13 bohrs in the distance from the C nucleus to the midpoint of the H - H axis. For the $^2B_1$ state in the reported region of the minimum energy path, R changes by 0.40 bohrs, while r changes by 0.66 bohrs.

Now we turn to a comparison of the present ab initio with the qualitative predictions of Mahan and Sloane, summarized in Fig. 1. Their predicted $^2A_1$ barrier is completely consistent with our results. However, for the $^2B_1$ state they predict no barrier, as opposed to the 63 kcal/barrier found here. In addition, Mahan and Sloane predict the $^2B_1$ state to be slightly chemically bound with respect to $C^+ + H_2$, while we find only a long range attraction. An important point emphasized by Mahan and Sloane concerns the fact that while the $^2A_1$ and $^2B_2$ surfaces cross each other in C_{2V} symmetry, these two states are both labeled $^2A'$ for general (C_S point group) geometry. Hence this crossing of C_{2V} potential surfaces becomes an avoided intersection for arbitrary approaches of C^+ to H_2. Thus the $^2A_1$ ground state of CH_2^+ can be reached adiabatically by $C^+(^2B_2) + H_2$ collisions. Figure 4 does indeed verify their qualitative conclusion that such an avoided intersection could occur at low relative energies. Note, however, that the "crossing point" in Fig. 2 of the $^2A_1$ and $^2B_2$ states is not the precise position of the surface crossing. This is because these two energy profiles are separately optimized with respect to r(H - H); and for a single value of R(C - X) there will be different values of r(H - H) for the $^2A_1$ and $^2B_2$ minimum energy paths.

$C_{\infty v}$ APPROACHES

Our results for linear CHH^+ approaches are summarized in Fig. 5, which shows approximate energy profiles for $C^+ + H_2 \rightarrow CH^+ + H$. The most obvious result is that the $^2\Sigma^+$ surface has a barrier while there is none for $C^+ + H_2 \rightarrow CH^+(^3\Pi) + H$. Note also that the long range attraction for the $^2\Sigma^+$ system must occur for $R \geqslant 5$ bohrs and be small relative to the well found for $^2\Pi$. The $^2\Pi$ long range attraction has its minimum for R(C - H) = 2.93 bohrs, r(H - H) = 1.50 bohrs, with well depth 8.2 kcal/mole.

Several points on the $^2\Sigma^+$ minimum energy path are shown in Table IV. Consistent with the Hammond postulate for endothermic reactions,[31] it is seen that the saddle point occurs closer to $CH^+(^1\Sigma^+) + H$ than to $C^+ + H_2$. The predicted barrier height for $C^+ + H_2 \rightarrow CH^+(^1\Sigma^+) + H$ is 28.4 kcal/mole. However, here we must remind the reader that our prediction of the endothermicity is 8.3 kcal/mole larger than experiment. Hence, we obtain a more reliable, but admittedly semi-empirical, value of 20.1 kcal/mole for the classical barrier height. For the exothermic reaction, $CH^+(^1\Sigma^+) + H \rightarrow C^+ + H_2$, no such correction is needed and our ab initio barrier height of 7.6 kcal/mole should be meaningful.

Mahan and Sloane predicted the same qualitative relationship between the $^2\Pi$ and $^2\Sigma^+$ energy profiles as seen in Fig. 5. That is, the $^2\Pi$ interaction is by far the more attractive. However, their figure indicates a somewhat larger potential well for $^2\Pi$ CHH^+ and no barrier for the $^2\Sigma^+$ reaction.

Perhaps the most intriguing aspect of Mahan and Sloane's discussion is their observation that "the lowest energy configuration ($^2\Pi$) of linear CHH^+ can evolve to the lowest energy configuration of CH_2^+." This can be illustrated by the orbital progression

$$3\sigma^2\ 1\pi \rightarrow 3a'^2 4a' \rightarrow 1b_2^2\ 3a_1$$

which accompanies the move from $C_{\infty V}$ to C_S to C_{2V} symmetry. Equally important, however, is the question of whether there is a barrier between the 8 kcal/mole $^2\Pi$ well and the much deeper $^2A_1$ CH_2^+ potential well. It might be argued that a large barrier cannot exist, since this would make it difficult to explain the molecular beam experiments--i.e. the apparent complex formation. Preferably, although beyond the scope of the present work, one might obtain ab initio the minimum energy path connecting these two potential wells.

CONCLUDING REMARKS

The present study represents a first step in the quest for an ab initio theoretical understanding of the dynamics of the $C^+ - H_2$ reaction. It seems very likely that this will be only the first chapter in a continuing study of this fascinating ion-molecule reaction. We also anticipate and openly encourage additional molecular beam studies, particularly at somewhat lower energies than reported to date.

A number of features of the ab initio CH_2^+ potential surface differ qualitatively from the intuitive correlation diagram of Mahan and Sloane. However, none of these features are crucial to the latter's discussion of the $C^+ + H_2$ dynamics. Necessary conditions for the plausibility of two pathways ($^2B_2 \rightarrow {}^2A' \rightarrow {}^2A_1$ and $^2\Pi \rightarrow {}^2A' \rightarrow {}^2A_1$) which might lead to complex formation have been satisfied. However, a detailed theoretical study of the C_s part of the potential surface is required to determine whether or not barriers exist along these pathways.

One ultimate goal of detailed quantum mechanical studies, such as this one, is to develop fundamental insight concerning the shapes of potential energy surfaces. In this light, the present work shows in a quantitative way the validity of the Woodward-Hoffman concept,[10] as discussed by Mahan,[5] for ion-molecule reactions. Our result for the $^2\Sigma^+$ state indicates that even when orbital symmetry is not a constraint, exothermic ion-molecule surfaces may contain barriers, in this case 7.6 kcal/mole. Such insights will become particularly valuable in cases where detailed computations are not feasible.

ACKNOWLEDGMENTS

This research was supported by the National Science Foundation, Grant GP-31974. We thank Professor Bruce H. Mahan for suggesting this study and for many helpful discussions. Valuable discussions with Dr. Thompson M. Sloane are also acknowledged.

FOOTNOTES AND REFERENCES

*Work performed under the auspices of the U. S. Atomic Energy Commission.

†M. H. Fellow. Present address: Lawrence Livermore Laboratory, University of California, Livermore, California 94550.

††Alfred P. Sloan Fellow.

1. J. Durbin and M. J. Henchman, in MPT International Review of Science, ed. by J. C. Polanyi (Butterworth's, London, 1972), Physical Chemistry Series One, Vol. 9.

2. R. Wolfgang, Accounts Chem. Res. 3, 48 (1970).

3. W. B. Maier, J. Chem. Phys. 46, 4991 (1967).

4. C. R. Iden, R. Liardon, W. Liardon, and W. S. Koski, J. Chem. Phys. 54, 2757 (1971); 56, 851 (1972).

5. B. H. Mahan, J. Chem. Phys. 55, 1436 (1971).

6. E. Lindemann, L. C. Frees, R. W. Rozett, and W. S. Koski, J. Chem. Phys. 56, 1003 (1972).

7. B. H. Mahan and T. M. Sloan, "Dynamics of the $C^+ - H_2$ Reaction", to be published.

8. G. Herzberg, Can. J. Phys. 39, 511 (1961).

9. C. F. Bender and H. F. Schaefer, J. Mol. Spect. 37, 423 (1971).

10. R. B. Woodward and R. Hoffmann, The Conservation of Orbital Symmetry (Academic Press, New York, 1970).

11. T. P. Schafer, P. E. Siska, J. M. Parson, F. P. Tully, Y. C. Wong, and Y. T. Lee, J. Chem. Phys. 53, 3385 (1970).

12. J. C. Polanyi and K. B. Woodall, J. Chem. Phys. 57, 1574 (1972).

13. R. D. Coombe and G. C. Pimentel, J. Chem. Phys. 59, 1535 (1973).

14. J. T. Muckerman, J. Chem. Phys. 57, 3388 (1972).

15. N. C. Blais and D. G. Truhlar, J. Chem. Phys. 58, 1090 (1973).

16. G. G. Schatz, J. M. Bowman, and A. Kuppermann, J. Chem. Phys. 58, 4023 (1973).

17. C. F. Bender, S. V. O'Neil, P. K. Pearson, and H. F. Schaefer, Science 176, 1412 (1972).

18. R. K. Preston and J. C. Tully, J. Chem. Phys. 54, 4297 (1971); 55, 562 (1971).

19. S. Huzinaga, J. Chem. Phys. 42, 1293 (1965).

20. T. H. Dunning, J. Chem. Phys. 53, 2823 (1970).

21. H. F. Schaefer, The Electronic Structure of Atoms and Molecules: A Survey of Rigorous Quantum Mechanical Results (Addison Wesley, Reading, Massachusetts, 1972).

22. A. D. Walsh, J. Chem. Soc. 2266 (1953).

23. G. Herzberg and J. W. Johns, Proc. Roy. Soc. (London) A295, 107 (1966).

24. P. O. Löwdin, Phys. Rev. 97, 1474 (1955).

25. C. F. Bender and E. R. Davidson, J. Phys. Chem. 70, 2675 (1966).

26. D. H. Liskow, C. F. Bender, and H. F. Schaefer, Lawrence Berkeley Laboratory Report LBL-2302, October 1973.

27. G. Herzberg and J. W. C. Johns, Astrophys. J. 158, 399 (1969).

28. W. Kolos and L. Wolniewicz, J. Chem. Phys. 49, 404 (1968).

29. S. Green, P. S. Bagus, B. Liu, A. D. McLean, and M. Yoshimine, Phys. Rev. A 5, 1614 (1972).

30. P. L. Moore, J. C. Browne, and F. A. Matsen, J. Chem. Phys. 43, 903 (1965).

31. G. S. Hammond, J. Am. Chem. Soc. 77, 334 (1955).

Table I. Energies of reactants, intermediates, and products of the $C^+ + H_2 \rightarrow CH^+ + H$ reaction.

$C^+(^2P_u) + H_2(^1\Sigma_g^+)$	E = -38.4843 hartrees	0.0 kcal/mole
$CH_2^+(^2A_1)$	E = -38.6152 hartrees	-82.1 kcal/mole
$CH_2^+(^2B_1)$	E = -38.6104 hartrees	-79.1 kcal/mole
$CH_2^+(^2B_2)$	Not chemically bound. See text.	
$CH^+(^1\Sigma^+) + H$	E = -38.4514 hartrees	+20.8 kcal/mole
$CH^+(^3\Pi) + H$	E = -38.4221 hartrees	+39.0 kcal/mole

Table II. Stationary points on the CH_2^+ C_{2V} potential energy surfaces. Saddle points refer to the processes $C^+ + H_2 \rightarrow CH_2^+$. Energies are given in kcal/mole relative to separated $C^+ + H_2$, and also in hartrees. Bond distances are in bohr radii (1 bohr = 0.5292 Å).

Symmetry	Geometry	Nature	Energy
$^2A_1$	R = 2.94, r = 2.34	Saddle point	85.7 (-38.3479)
$^2B_1$	R = 3.66, r = 1.46	Long range attraction	-7.3 (-38.4959)
$^2B_1$	R = 2.33, r = 3.00	Saddle point	62.8 (-38.3842)
$^2B_2$	R = 3.34, r = 1.49	Long range attraction	-8.3 (-38.4975)

Table III. C_{2V} minimum energy paths near the saddle point for $C^+ + H_2 \rightarrow CH_2^+$. Bond distances are given in bohrs and energies in kcal/mole relative to separated $C^+ + H_2$.

$C^+ + H_2 \quad {}^2A_1 \; CH_2^+$

R(C - X)	r(H - H)	Energy	Comments
∞	1.40	0.0	Reactants
2.96	2.07	76.8	
2.95	2.21	82.1	
2.95	2.30	84.5	
2.94	2.34	85.6	Saddle point
2.89	2.34	85.4	
2.87	2.39	84.0	
2.85	2.52	77.6	
2.83	2.57	74.5	
0.71	3.93	-82.1	Product

$C^+ + H_2 \rightarrow {}^2B_1 \; CH_2^+$

R(C - X)	r(H - H)	Energy	Comments
∞	1.40	0.0	Reactants
2.51	2.54	47.9	
2.43	2.74	56.7	
2.38	2.87	61.1	
2.33	3.00	62.8	Saddle point
2.26	3.05	61.6	
2.20	3.13	58.4	
2.11	3.20	51.9	
0.00	4.16	-79.1	Product

Table IV. $^{2+}$ minimum energy path for $C^+ + H_2 \rightarrow CH^+(^1\Sigma^+) + H$ near the saddle point. Bond distances are in bohrs and energies in kcal/mole relative to separated $C^+ + H_2$.

R(C - H)	r(H - H)	Energy	Comments
∞	1.40	0.0	Reactants
2.87	1.42	20.4	
2.71	1.64	24.1	
2.57	1.95	27.9	
2.51	2.11	28.4	Saddle point
2.46	2.27	27.9	
2.41	2.41	27.1	
2.17	∞	20.8	Products

FIGURE CAPTIONS

Fig. 1. Correlation diagram of Mahan and Sloane[7] for $C^+ + H_2 \rightarrow CH^+ + H$.

Fig. 2. Coordinate system for C_{2V} geometries.

Fig. 3. Coordinate system for $C_{\infty V}$ geometries.

Fig. 4. Energy profiles along the C_{2V} minimum energy paths for $C^+ + H_2 \rightarrow CH_2^+$.

Fig. 5. Energy profiles along the minimum energy paths for linear $C^+ + H_2 \rightarrow CH^+ + H$.

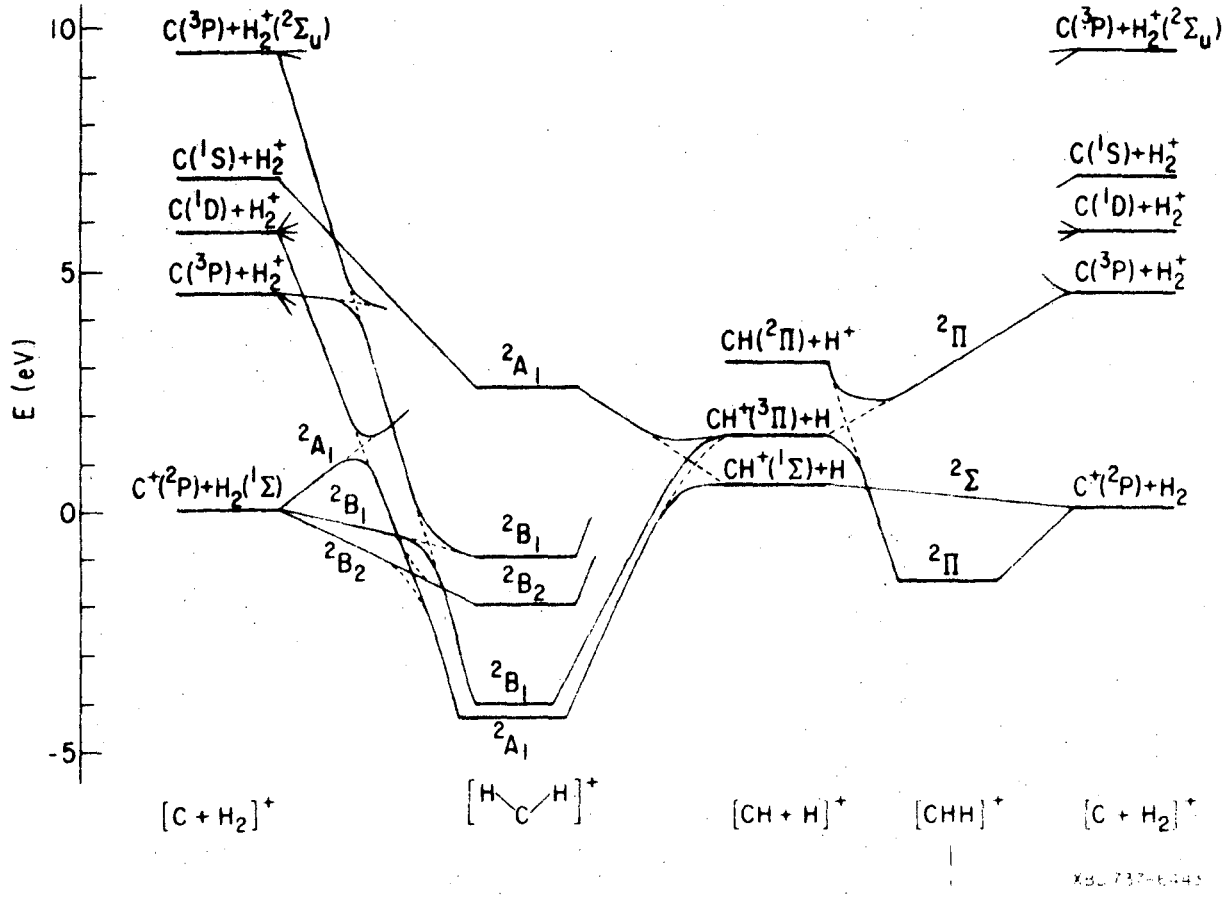
10
5
0
-5
E (eV)
C(3P)+H2+(2Σu)
C(1S)+H2+
C(1D)+H2+
C(3P)+H2+
2A1
2A1
C+(2P)+H2(1Σ)
2B1
2B2
2B1
2B2
2B1
2A1
CH(2Π)+H+
CH+(3Π)+H
CH+(1Σ)+H
2Π
2Σ
2Π
C(3P)+H2+
C(1S)+H2+
C(1D)+H2+
C+(2P)+H2
[C + H2]+
[H C H]+
[CH + H]+
[CHH]+
[C + H2]+

Fig. 1

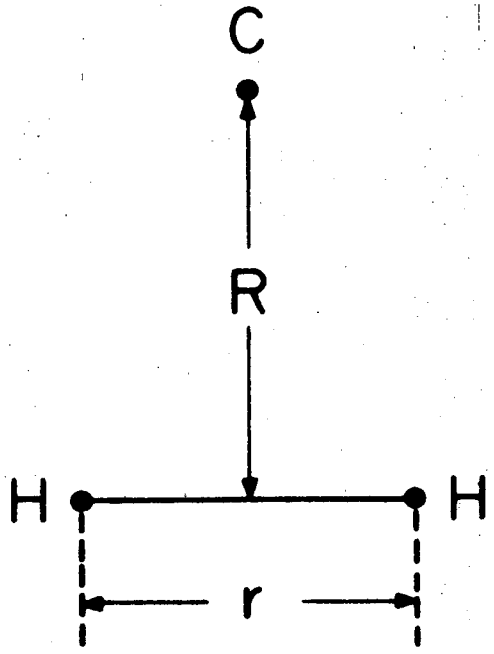

C_{2v} Geometries

XBL739-4046

Fig. 2

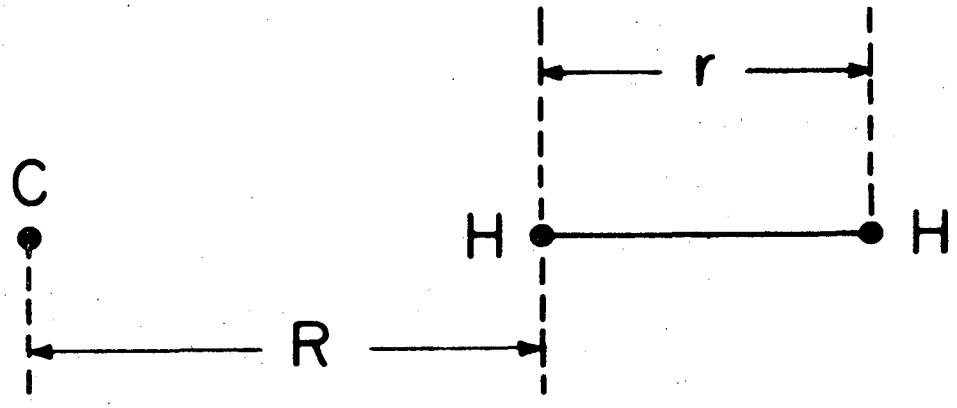

$C_{\infty v}$ Geometries

XBL739-4045

Fig. 3

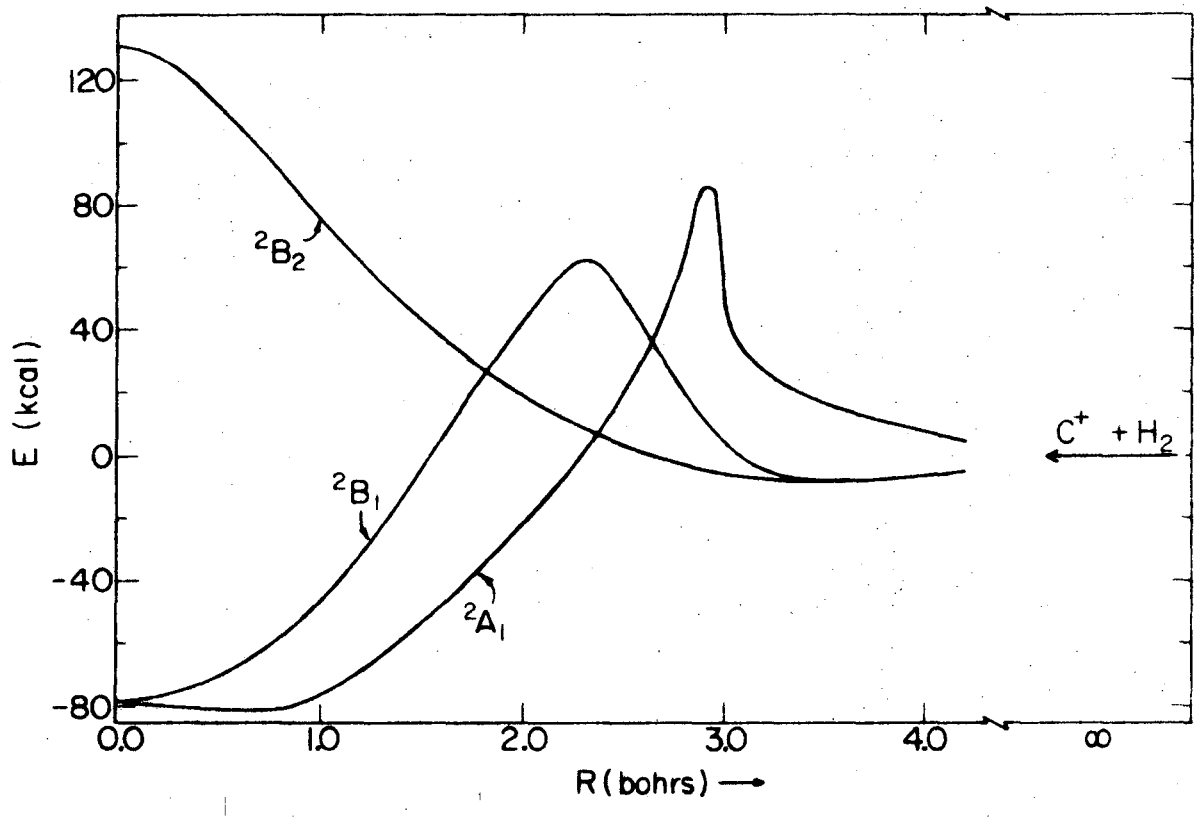
120
80
40
0
-40
-80
E (kcal)
0.0
1.0
2.0
3.0
4.0
∞
R (bohrs) ⟶
$^2B_2$
$^2B_1$
$^2A_1$
$C^+ + H_2$
7310-4163

Fig. 4

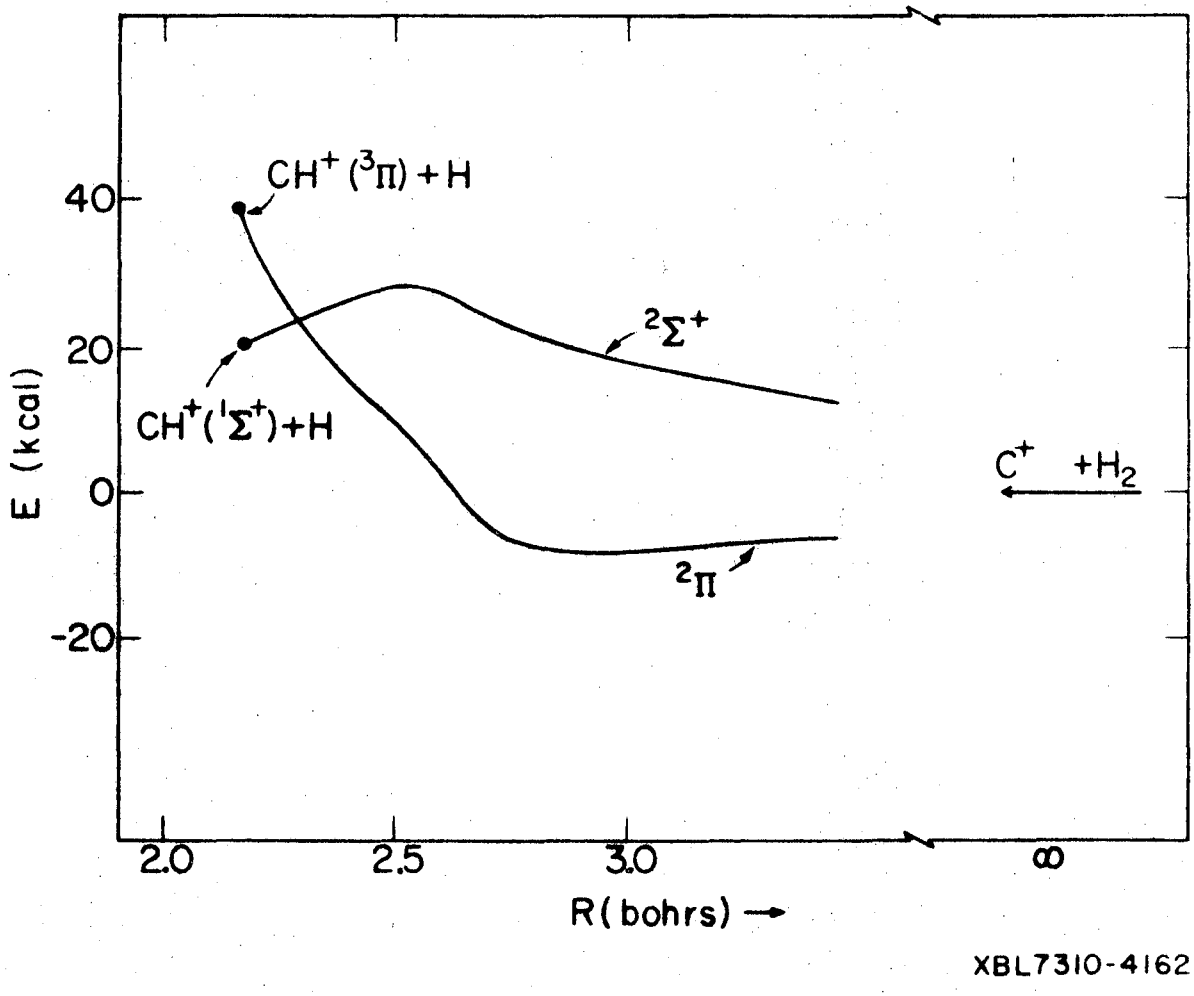
CH+ (3Π) + H
40
20
0
-20
E (kcal)
CH+(1Σ+)+H
2Σ+
2Π
C+ +H2
2.0
2.5
3.0
∞
R(bohrs) →
XBL7310-4162

Fig. 5

R(CX)	R(HH)	E(AU)
0.0	4.080	-38.609730
0.7100	3.933	-38.615192
1.0	3.0	-38.561020
2.0	1.4	-38.351094
2.0	1.6	-38.390519
2.0	1.8	-38.421299
2.0	2.1	-38.456698
2.0	2.0	-38.446120
2.0	2.2	-38.466175
2.0	2.6	-38.494162
2.0	2.8	-38.502796
2.0	3.0	-38.508285
2.0	3.2	-38.510964
2.0	3.4	-38.511177
2.4	1.4	-38.322088
2.4	1.6	-38.350815
2.4	1.8	-38.372930
2.4	2.0	-38.391170
2.4	2.2	-38.406567
2.6	1.2	-38.322064
2.6	1.4	-38.333193
2.6	1.6	-38.333895
2.6	1.8	-38.347282
2.6	2.0	-38.362456
2.6	2.2	-38.376377
2.6	2.4	-38.388545
2.6	2.6	-38.398831
2.6	2.8	-38.407160
2.8	1.2	-38.363575
2.8	1.4	-38.373501
2.8	1.6	-38.368891
2.8	1.8	-38.358160
2.8	2.0	-38.347923
2.8	2.2	-38.349567
2.8	2.4	-38.360807
2.8	2.6	-38.370870
2.8	2.8	-38.379357
2.8	3.2	-38.391323
2.8	3.6	-38.397007
2.9	2.2	-38.349493
2.9	2.4	-38.347743
2.9	2.6	-38.357884
2.94	2.34	-38.347857
3.0	1.2	-38.394663
3.0	1.3	-38.402134
3.0	1.4	-38.404408
3.0	1.6	-38.399299
3.0	1.8	-38.387429
3.0	2.0	-38.373337
3.0	2.2	-38.359776
3.0	2.4	-38.349736
3.0	2.6	-38.344084

3.0	2.8	-38.353472
3.0	3.0	-38.360402
3.0	3.2	-38.365741
3.0	3.6	-38.372466
3.2	2.4	-38.366438
3.2	2.6	-38.354938
3.2	2.8	-38.347294
3.2	3.2	-38.342817
4.0	1.35	-38.471522
4.0	1.4	-38.472226
4.0	1.45	-38.471997
10.0	1.4	-38.484486
100.	1.4	-38.484342

(BOND DISTANCES IN ATOMIC UNITS 1 AU = .5292 ANGSTROM)

*** CH2+ 2B1 ***

R(CX)	R(HH)	E(AU)
0.0	4.080	-38.609765
0.0	4.160	-38.610401
1.0	3.0	-38.489501
2.0	2.0	-38.376153
2.0	2.2	-38.374165
2.0	2.4	-38.377780
2.0	2.6	-38.387012
2.0	2.8	-38.397964
2.0	3.0	-38.407955
2.0	3.2	-38.415963
2.0	3.4	-38.421760
2.15	2.63	-38.383687
2.2	2.2	-38.398659
2.2	2.4	-38.390148
2.2	2.6	-38.385277
2.2	2.8	-38.383928
2.2	3.0	-38.387938
2.2	3.2	-38.392370
2.33	3.00	-38.384202
2.4	1.6	-38.453220
2.4	1.8	-38.444545
2.4	2.0	-38.432627
2.4	2.2	-38.419956
2.4	2.4	-38.408019
2.4	2.6	-38.397787
2.4	2.8	-38.389967
2.4	3.0	-38.384970
2.4	3.2	-38.382670
2.6	2.4	-38.422333
2.6	2.6	-38.410445
2.6	2.8	-38.400117
2.6	3.0	-38.391623
2.6	3.2	-38.385101
2.8	2.4	-38.432416
2.8	2.6	-38.419945
2.8	2.8	-38.408686
2.8	3.0	-38.398836
2.8	3.2	-38.390500
2.8	3.6	-38.378401
3.0	1.4	-38.488739
3.33	3.00	-38.408279
3.4	1.4	-38.494557
3.4	1.5	-38.495103
3.4	1.6	-38.492988
3.6	1.3	-38.491094
3.6	1.4	-38.495301
3.6	1.5	-38.495727
3.6	1.6	-38.493504
3.8	1.4	-38.495247
3.8	1.5	-38.495525
4.0	1.4	-38.494702
10.0	1.4	-38.485276

100. 1.4 -38.485119

(BOND DISTANCES IN ATOMIC UNITS 1 AU = .5292 ANGSTROM)

*** CH2+ 282 ***

R(CX)	R(HH)	E(AU)
0.0	4.080	-38.275376
0.704	3.85	-38.322405
0.7182	3.946	-38.331163
1.0	3.0	-38.294753
1.0500	3.637	-38.370575
1.3499	3.217	-38.405766
2.0	1.8	-38.459735
2.0	2.2	-38.464903
2.0	2.4	-38.464862
2.0	2.6	-38.463612
2.0	2.8	-38.461296
2.0	3.0	-38.458005
2.0	3.2	-38.453825
2.2	1.6	-38.473196
2.2	1.8	-38.475803
2.2	2.0	-38.475094
2.2	2.2	-38.472823
2.2	2.4	-38.469741
2.2	2.6	-38.466109
2.2	2.8	-38.461982
2.2	3.0	-38.457350
2.2	3.2	-38.452211
2.4	1.4	-38.478227
2.4	1.6	-38.484340
2.4	1.8	-38.483414
2.4	2.0	-38.479431
2.4	2.2	-38.474321
2.4	2.4	-38.468918
2.4	2.6	-38.463491
2.4	2.8	-38.458043
2.6	1.2	-38.467997
2.6	1.4	-38.486762
2.6	1.6	-38.490394
2.6	1.8	-38.486901
2.6	2.0	-38.480402
2.6	2.2	-38.472970
2.6	2.4	-38.465553
2.6	2.6	-38.458488
2.8	1.4	-38.491792
2.8	1.6	-38.493725
2.8	1.8	-38.488406
2.8	2.0	-38.480020
2.8	2.2	-38.470716
2.8	2.4	-38.461537
3.0	1.2	-38.478497
3.0	1.4	-38.494657
3.0	1.6	-38.495418
3.0	1.8	-38.488822
3.2	1.5	-38.497346
3.4	1.4	-38.496510
3.4	1.5	-38.497451
3.4	1.6	-38.495769

3.6	1.3	-38.491842
3.6	1.4	-38.496264
3.6	1.5	-38.496928
3.6	1.6	-38.494965
4.0	1.4	-38.494624
10.0	1.4	-38.484373
100.	1.4	-38.484211

(BOND DISTANCES IN ATOMIC UNITS 1 AU = .5292 ANGSTROM)

*** CH2+ 2SIG ***

R(CH)	R(HH)	E(AU)
2.0	1.6	-38.385790
2.0	2.4	-38.429669
2.1	2.2	-38.431165
2.130	100.	-38.451125
2.136	100.	-38.451198
2.142	100.	-38.451260
2.148	100.	-38.451311
2.154	100.	-38.451351
2.166	100.	-38.451400
2.178	100.	-38.451408
2.2	2.0	-38.430509
2.2	2.4	-38.440461
2.3	1.8	-38.429587
2.3	2.2	-38.438606
2.4	1.6	-38.429156
2.4	2.0	-38.437344
2.4	2.4	-38.441317
2.5	1.4	-38.426677
2.5	1.8	-38.438188
2.5	2.2	-38.439217
2.6	1.2	-38.413670
2.6	1.6	-38.440940
2.6	2.0	-38.439687
2.6	2.4	-38.437402
2.7	1.4	-38.441412
2.7	1.8	-38.443791
2.7	2.2	-38.436889
2.8	1.6	-38.449952
2.8	2.0	-38.440398
2.8	2.4	-38.431652
2.9	1.4	-38.452768
2.9	1.8	-38.448197
2.9	2.2	-38.433827
3.0	1.6	-38.457158
3.0	2.0	-38.441066
3.1	1.4	-38.461524
3.1	1.8	-38.452065
3.2	1.6	-38.462963
3.3	1.4	-38.468202
9.3	1.4	-38.484218
99.3	1.4	-38.484210

(BOND DISTANCES IN ATOMIC UNITS 1 AU = .5292 ANGSTROM)

*** CH2+ 2PI ***

R(CH)	R(HH)	E(AU)
2.0	1.6	-38.455975
2.0	2.4	-38.441422
2.1	1.4	-38.463403
2.124	100.	-38.421998
2.130	100.	-38.422046
2.136	100.	-38.422086
2.142	100.	-38.422114
2.148	100.	-38.422132
2.154	100.	-38.422141
2.166	100.	-38.422129
2.2	1.6	-38.478090
2.2	2.8	-38.444372
2.2	3.2	-38.436672
2.2	3.6	-38.431354
2.2	4.0	-38.427798
2.2	4.4	-38.425488
2.2	4.8	-38.424095
2.3	1.4	-38.480911
2.4	1.6	-38.489193
2.4	2.4	-38.460352
2.5	1.4	-38.489982
2.6	1.2	-38.475643
2.6	1.6	-38.494093
2.6	2.0	-38.479369
2.6	2.4	-38.459539
2.7	1.4	-38.494237
2.8	1.2	-38.479510
2.8	1.6	-38.495605
2.8	2.4	-38.455634
2.9	1.4	-38.495787
2.9	1.8	-38.488045
3.0	1.2	-38.481186
3.0	1.6	-38.495280
3.1	1.4	-38.495856
3.1	1.8	-38.486221
3.2	1.2	-38.481625
3.2	1.6	-38.494037
3.3	1.4	-38.495160
3.4	1.2	-38.481381
9.3	1.4	-38.484229
99.3	1.4	-38.484277

(BOND DISTANCES IN ATOMIC UNITS 1 AU = .5292 ANGSTROM)

TECHNICAL INFORMATION DIVISION
LAWRENCE BERKELEY LABORATORY
UNIVERSITY OF CALIFORNIA
BERKELEY, CALIFORNIA 94720